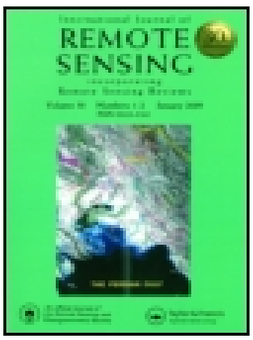

International Journal of Remote Sensing

ISSN: 0143-1161 (Print) 1366-5901 (Online) Journal homepage: http://www.tandfonline.com/loi/tres20

Variability of aerosol optical thickness in the tropical Indian Ocean and South China Sea during spring intermonsoon season

Qingyang Sun, DanLing Tang, Gad Levy & Ping Shi

To cite this article: Qingyang Sun, DanLing Tang, Gad Levy & Ping Shi (2017): Variability of aerosol optical thickness in the tropical Indian Ocean and South China Sea during spring intermonsoon season, International Journal of Remote Sensing, DOI: 10.1080/01431161.2017.1387310

To link to this article: http://dx.doi.org/10.1080/01431161.2017.1387310

INTERNATIONAL JOURNAL OF REMOTE SENSING, 2017
https://doi.org/10.1080/01431161.2017.1387310

Taylor & Francis
Taylor & Francis Group

Variability of aerosol optical thickness in the tropical Indian Ocean and South China Sea during spring intermonsoon season

Qingyang Sun[a,b], DanLing Tang[b,c], Gad Levy[d] and Ping Shi[b]

[a]South China Sea Institute of Planning and Environmental Research, State Oceanic Administration, Guangzhou, China; [b]State Key Laboratory of Tropical Oceanography (LTO), Guangdong Key Laboratory of Ocean Remote Sensing (LORS), South China Sea Institute of Oceanology, Chinese Academy of Sciences, Guangzhou, China; [c]Collaborative Innovation Center for 21st-Century Maritime Silk Road Studies, Guangzhou, China; [d]NorthWest Research Associates, Seattle, WA, USA

ABSTRACT

The variability of aerosol optical thickness (AOT) in the tropical Indian Ocean (IO) and South China Sea (SCS) during the intermonsoon (February–May) is investigated using shipboard and satellite data from 2011 to 2014, in order to understand the mechanism controlling AOT production and transport. Overall AOT in tropical IO is significantly smaller than those in SCS, and a strong intraseasonal variability of AOT, along with significant dependence on wind speed (especially when <8 m s^{-1}), is observed in both basins. Our analysis showed that in tropical IO, aerosols are mostly of natural marine production in spring, and the AOT shows greater dependence on the higher wind speeds in May, while in SCS, AOT dependence on wind speed increases when the prevailing wind turns from offshore (February, March) to onshore (April, May), due to less transport of terrestrial dust and anthropogenic aerosols from land. A better agreement between shipboard and once-daily satellite AOT is observed in the Equatorial belt (5° S–5° N, i.e. remote areas of IO) than in the Non-Equatorial area (5° N–25° N), and can be explained by the overall lower AOT values and the smaller diurnal variation in the Equatorial belt. Changes of wind regime during the monsoon evolution and the consequent transport of land-based aerosols reduce AOT dependence on wind speed and are the major drivers for the AOT variability.

ARTICLE HISTORY
Received 4 February 2017
Accepted 24 September 2017

1. Introduction

Aerosol observations are essential for understanding the Earth's radiation budget and the complexities of climate and climate change, as they contribute significantly to reflecting/absorbing solar radiation directly and they modify cloud properties indirectly (Charlson et al. 1992; Penner, Dickinson, and Oneill 1992; Liepert and Tegen 2002), thereby causing net cooling of the Earth surface and spinning down the water cycle (Ramanathan et al. 2001a;

CONTACT Danling Tang lingzistdl@126.com State Key Laboratory of Tropical Oceanography (LTO), Guangdong Key Laboratory of Ocean Remote Sensing (LORS), South China Sea Institute of Oceanology, Chinese Academy of Sciences, Guangzhou, China

Liepert et al. 2004). Aerosols are also important when studying marine biogeochemistry, through their contribution to blocking the solar radiation, increasing cloudiness and cloud liquid water, which reduce the daytime solar heating and moderate the diurnal temperature range (Hansen, Sato, and Ruedy 1995; Dai, Trenberth, and Karl 1999; Barnett, Adam, and Lettenmaier 2005; Huang, Dickinson, and Chameides 2006); their provision of nutrients, which enhance biological productivity and promote nitrogen fixation in the oceans (de Baar et al. 1995; Capone et al. 1997; Paerl 1997; Timmermans et al. 2001; Yuan and Zhang 2006); thus indirectly altering the phytoplankton community structure and growth rate in marine ecosystems (Paerl 1997; Guo et al. 2012).

The aerosol optical thickness (AOT), defined as the degree to which aerosols prevent the transmission of light, has been widely observed and studied, both from ground observations (Smirnov et al. 1995; 2003a; 2003b; Smirnov et al. 2012; Holben et al. 1998; Mulcahy et al. 2008) and satellite remote sensing products (Remer, Kaufman, and Kleidman 2006; Zhang and Reid 2006; Lee et al. 2007; Lin et al. 2007). The oceanic aerosol loading is influenced by meteorological factors such as the wind speed and the availability of moisture (Fitzgerald 1991; Smirnov et al. 1995), and the relationship between marine aerosols and sea surface wind speed has been studied in numerous studies (e.g. see Table 3 from Smirnov et al. 2012). It has been found that the maritime AOT increases in tandem with increases in near-surface wind speeds: as the wind increases so do the fluxes of sea spray (i.e. increased aerosol mass), and water vapour (i.e. aerosol swelling) from the ocean to the marine boundary layer (Smirnov et al. 2003b; Mulcahy et al. 2008; Glantz, Nilsson, and Von Hoyningen-Huene 2009; Kiliyanpilakkil and Meskhidze 2011).

The present study is made in the tropical Indian Ocean (IO) and the South China Sea (SCS), where the climate is affected greatly by monsoons. The SCS, one of the largest marginal seas of the world (Liu et al. 2002; Tseng et al. 2005), is influenced by Asian monsoon: northeast in winter and southwest in summer (Lau and Yang 1997; Chen, Graf, and Huang 2000; Ding and Chan 2005). Bounded by the shelves along the southern coasts of China and the Sunda Shelf that further stretches to the Gulf of Thailand, the SCS receives aerosols from land based sources that can come from the north, west and south. These advected aerosols have great impacts on marine biogeochemistry and marine ecosystems (Lin et al. 2007; Lin et al. 2009; Wong et al. 2007; Guo et al. 2012). In the tropical IO, the AOT near the Equator is low throughout the year, and its properties show large spatial differences between the northern hemisphere and the southern hemisphere (Moorthy, Satheesh, and Murthy 1997; DeWitt et al. 2013; Salim and Mishra 2013). Anthropogenic aerosols transported from the Indian subcontinent and surrounding areas during the northeast (winter) monsoon play an important role in determining aerosol properties and distributions in northern IO (Ramanathan et al. 2001b; Li and Ramanathan 2002; Menon et al. 2011). Aerosols over tropical IO also showed large dependency on wind speed (Moorthy, Satheesh, and Murthy 1997), especially when the Madden-Julian Oscillation (MJO) was present (DeWitt et al. 2013), as well as a strong positive correlation with water vapor (Salim and Mishra 2013).

Previous studies found that the distribution and variability of AOT are related to the active monsoon season in tropical IO and SCS. However, how AOT respond to the origination of monsoon during the intermonsoon season in both basins has not been well studied previously. The main objective of the present study is to explore the variability of AOT in the tropical IO and the SCS during the transition from winter to

summer monsoon in response to the summer monsoon arrival, and to understand the mechanisms that control this variability. Both shipboard and satellite datasets in both basins are analysed in this study and the shipboard measurements are further applied to validate satellite retrieved AOT products in the research area.

2. Data and methods

2.1. *In situ measurements*

We participated in research cruises organized by the South China Sea Institute of Oceanology (SCSIO), Chinese Academy of Sciences, in the SCS and the East IO during the intermonsoon (February–May) from 2011 to 2014. The shipboard AOT measurements were collected with two portable, hand-held Microtops II sun photometers, designed by Solar Light Inc. and widely used by researchers throughout the world (Morys et al. 2001; Smirnov et al. 2009). One photometer with five channel configuration (380, 500, 675, 936, and 1020 nm) was used to collect the AOT data from 2011 to 2013, but required calibration in 2014, and therefore was replaced by another photometer equipped with a somewhat different channel configuration (440, 500, 675, 870, and 1020 nm) in 2014. Considering the satellite transit time (for comparison of ship measurements and satellite data in Section 2.2), as well as the propagation distance of light (longer in sunrise and sunset than in the noon), measurements of AOT alongside the weather conditions were designed to be taken four times a day at about 6:00 (sunrise), 8:00, 14:00, and 17:30 (sunset, local time), strictly following the procedures and precautions suggested by Porter et al. (2001). At least 10 measurements were made each time, all within 5 min (including turning the unit off and on for dark correction), and the minima of these measurements were collected as the true value for each observation. Measurements of the two photometers were cross-calibrated. The data were also processed to mitigate the drift in instrument performance and cross-calibrated with the Maritime Aerosol Network (MAN), of which they became part of, following the Aerosol Robotic Network (AERONET) procedures (Smirnov et al. 2009; data are available on the MAN website: http://aeronet.gsfc.nasa.gov/new_web/maritime_aerosol_network.html).

The MAN transfer calibration procedure resulted in the removal of measurements in the water vapour channel (936 nm) and some other drift channels (380 nm degraded in 2012 and 2013 and out of band leakage in 440 nm in 2014). Further quality control and data processing protocols are made for the analysis: first, all measurements above 1 were removed, as those account for the majority of the user error; second, data recorded during very heavy cloud cover were discarded; finally, the remaining data that were not within two standard deviations of the mean AOT were marked as outliers.

2.2. *Comparison of shipboard and satellite AOT data*

Due to the limited shipboard samples, satellite datasets are used for the analysis of large-scale variability in the present study. Widely used Level-3 daily aerosol products of the Moderate Resolution Imaging Spectroradiometer (MODIS) on board Aqua at 869 nm with 25 km spatial resolution (Remer et al. 2002; available from National Aeronautics and Space Administration Ocean Colour website: http://oceancolor.gsfc.nasa.gov/) were used

for comparison with our shipboard measurements. Daily sea surface wind vectors (~10 m above the sea surface) with a 25 km spatial resolution from the Advanced Scatterometer (ASCAT) provided by Remote Sensing Systems (Figa-Saldaña et al. 2002; Ricciardulli, Meissner, and Wentz 2012; available at http://www.remss.com/) were used to explore the relationship between AOT and wind regime.

After processing, calibration, and quality control protocols were applied, four channels (380, 500, 675, and 1020 nm) in 2011, three channels (500, 675, and 1020 nm) in 2012 and 2013, and four channels (500, 675, 870, and 1020 nm) are left in our shipboard measurements. Measurements in 2014 are compared to MODIS-Aqua 869 nm products directly in the present study, since the 870 nm channel is very close to the MODIS wavelength channel. However, there is no channel in 2011–2013 data which is very close to the satellite band, so an interpolation is needed for shipboard measurements to get the AOT at 869 nm. A second-order polynomial fit with a logarithmic operation was used to make the adjustment (Eck et al. 1999):

$$\ln(\tau) = a_0 + a_1 \ln\lambda + a_2 (\ln\lambda)^2, \tag{1}$$

where τ is the corresponding AOT value at the wavelength λ, and a_0,a_1 and a_2 are constants that need to be determined. For each measurement with at least three AOT values (τ) at different wavelengths, one can estimate a_0, a_1, and a_2 using the polynomial fit and direct minimization. Hence, for 2011–2013, the AOT at 869 nm are derived using Equation (1).

Because of the limited resolution and swath size of MODIS-Aqua, remote sensing AOT data were not always available directly over the location of the vessel. A *K*-nearest neighbour algorithm (k = 8) was used in the present study to match the most recent MODIS-Aqua AOT field for each ground based measurement (Friedman, Bentley, and Finkel 1977). Due to limited MODIS coverage at low latitudes, occasionally interpolation was carried out over a very large distance. A threshold distance of 100 km was used to spatially limit the interpolation for the satellite datasets (Ichoku et al. 2002). The matched MODIS-Aqua AOTs were then averaged after using a normalized inverse distance squared weight function (Levy and Brown 1986):

$$\begin{aligned} W_i &= \frac{R^2 - r_i^2}{R^2 + r_i^2}, \ r_i \le R \\ W_i &= 0, \ r_i > R, \end{aligned} \tag{2}$$

where r_i is the distance between a matched satellite pixel and the ground based measurement, R is the threshold (100 km), and W_i is the weight, which decreases monotonously from 1.0 at r_i = 0 to 0 at $r_i = R$.

3. Results

3.1. *Spatial and intraseasonal variability of shipboard AOT measurements*

The shipboard AOT measurements left after these processing procedures and used in the present study are shown in Figure 1. Most of the observations are located in the SCS and IO (measurements very close to land are removed), and the data were collected during March–May, 2011, February–April, 2012, April–May, 2013, and April–May, 2014.

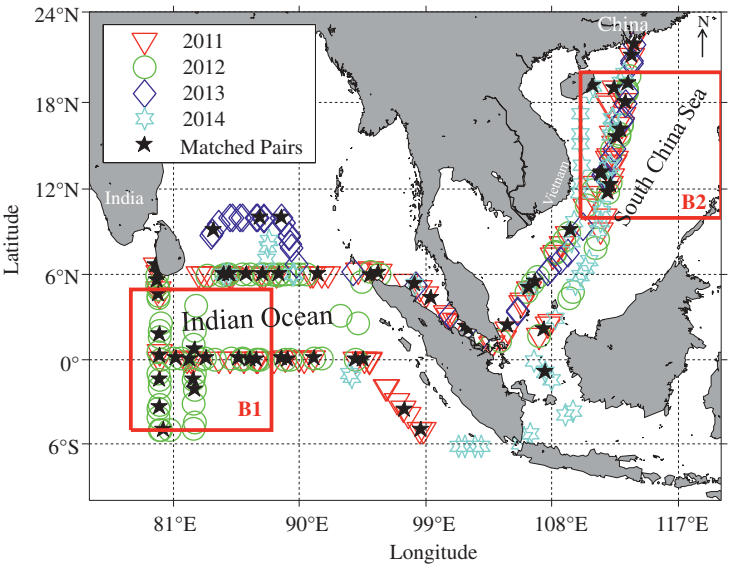

Figure 1. Map showing the distribution of shipboard AOT measurements in 2011 (red inverted triangle), 2012 (green circle), 2013 (blue rhombus), and 2014 (cyan hexagon) Indian Ocean Cruise, and the spatial distribution of matched pairs (black star) of shipboard and MODIS-Aqua AOT measurements. The two red boxes indicate the satellite collected data study areas in the South China Sea (SCS, box 'B1') and the tropical Indian Ocean (IO, box 'B2'), and area between the two blue lines indicate the Equatorial belt.

Statistically significant (spatial) difference of the mean AOT was observed from the shipboard observations based on observation location. Due to the significant variation in spatial distribution of the wind regimes (details in Section 3.3.1), we separated our research area into latitude belts (different than the basin-based separation of the IO and SCS): the belt near the Equator (hereafter 'Equatorial belt', i.e. 5° S–5° N, the area between the two blue lines in Figure 1, which includes the Equatorial IO and Java Sea) and the latitude belt farther away from the Equator (i.e. areas outside the two blue lines in Figure 1, containing measurements mostly in the South China Sea and the northern IO, hereafter 'Non-Equatorial area'). The mean AOT in the IO (AOT_{IO}) during spring season is 0.13 ± 0.01, while the mean value in SCS (AOT_{SCS}) is 0.16 ± 0.01, which is significantly higher than that in IO ($p = 0.04$, Table 1). The AOT in Equatorial belt (AOT_E) is lower (0.12 ± 0.01 vs. 0.16 ± 0.01) than that in Non-Equatorial area (AOT_{NE}), and the means are significantly different at the 0.05 level ($p = 0.01$, Table 1).

A clear intraseasonal variation was also evident in the shipboard observations (Table 2). The mean AOT showed a maximum in May (0.17 ± 0.01) and a minimum in February (0.12 ± 0.02). The diurnal variation (defined as the difference between the daily maxima and minima) and its spatial variability was also tested for. Smaller diurnal variation of AOT_{IO} than AOT_{SCS} (0.08 ± 0.02 vs. 0.11 ± 0.02), as well as AOT_E than AOT_{NE} (0.07 ± 0.01 vs. 0.10 ± 0.01, $p = 0.04$) were observed from shipboard measurements.

3.2. *Agreement of shipboard and satellite data*

With all the shipboard AOT observations quality controlled (details in Section 2.2) and collocated with MODIS-Aqua observations, 58 matched pairs (Figure 1, dark stars)

Table 1. Spatial difference of all shipboard AOT measurement and RMS difference between satellite and shipboard measurement ('$RMS_{Matched}$') from 2011 to 2014 (expressed as mean ± standard error).

Shipboard measurement		Sample size	AOT	*p*
All	AOT_E	76	0.12 ± 0.01	0.01
	AOT_{NE}	131	0.16 ± 0.01	
	AOT_{IO}	112	0.13 ± 0.01	0.04
	AOT_{SCS}	88	0.16 ± 0.01	
$RMS_{Matched}$	AOT_E	24	0.01 ± 0.002	≪0.05
	AOT_{NE}	34	0.03 ± 0.003	
	AOT_{IO}	30	0.02 ± 0.003	0.60
	AOT_{SCS}	28	0.02 ± 0.003	

'E' and 'NE' correspond to 'Equatorial' and 'Non-Equatorial', respectively. The *p*-values refer to statistical significance of differences between samples, and 0.05 is the critical value.

Table 2. The monthly mean value and the diurnal (the difference between the daily maxima and minima) variation of shipboard AOT measurement (mean ± standard error) in 2011–2014.

Shipboard measurement		Sample size	AOT	*p*
Monthly mean value	AOT_{Feb}	6	0.12 ± 0.02	0.09
	AOT_{Mar}	39	0.16 ± 0.01	
	AOT_{Apr}	113	0.13 ± 0.01	
	AOT_{May}	61	0.17 ± 0.01	
Diurnal variation	AOT_E	27	0.08 ± 0.02	0.31
	AOT_{NE}	39	0.10 ± 0.01	
	AOT_{IO}	38	0.07 ± 0. 01	0.04
	AOT_{SCS}	22	0.11 ± 0.02	

The *p*-values are the same as in Table 1.

remain. A linear correlation model (slope = 0.81, intercept = 0.02; R^2 = 0.80, $p \ll 0.05$) was fit between shipboard measurements and the data for all the data (Figure 2a, black line). When grouped as a function of distance from the equator, the agreement in AOT_E (Figure 2a red line; slope = 0.91, intercept = 0.01; R^2 = 0.86, $p \ll 0.05$) was better than that of AOT_{NE} (Figure 2a blue line; slope = 0.71, intercept = 0.04; R^2 = 0.75, $p \ll 0.05$). A

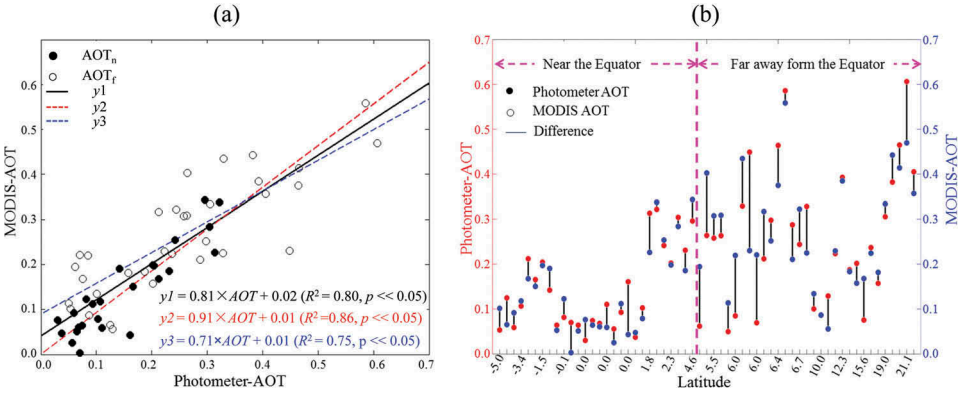

Figure 2. (*a*) Correlation between shipboard AOT measurements and MODIS-Aqua AOT products. The black solid line, red dashed, and blue dashed lines stand for the correlation of all matches (*y*1), matches of AOT_n (*y*2), and matches of AOT_f (*y*3), respectively. (*b*) The difference between shipboard measurements and satellite AOT data as a function of latitude.

significant spatial difference ($p \ll 0.05$) between AOT_E and AOT_{NE} is also reflected as in the agreement between *in situ* and satellite (Table 1 and Figure 2b; the RMS difference is 0.01 ± 0.002 and 0.03 ± 0.003, respectively).

In order to test whether there is a weather conditions related bias or deterioration in measurements and retrievals accuracy, the agreement between satellite and *in-situ* AOT measurements under different weather conditions was also tested using one-way ANOVA. There is no evidence of such bias or loss of accuracy: AOT measured and retrieved under sunny weather are not significantly different from those measured and retrieved in light cloudy weather ($p = 0.28$).

3.3. *Variability of AOT and wind regime during intermonsoon season from satellite*

Our shipboard AOT measurements were collected during the intermonsoon season. Considering the spatial difference revealed by our shipboard measurements and the agreement between shipboard and satellite observations ($R^2 = 0.89$, $p \ll 0.05$, Figure 2), we select two sampled areas in the tropical IO (5° S–5° N, 78° E–88° E, boxes 'B1' in Figures 1 and 3) and the SCS (10° N–20° N, 110° E–120° E, boxes 'B2' in Figures 1 and 3) as representative for further study and analysis with a larger dataset of satellite observations.

3.3.1. *Variability of AOT and wind regimes during monsoon evolution*

From the monthly average satellite wind products for the intermonsson – February, March, April and May from 2011 to 2014 (Figure 3), one can discern a distinct turnover of the prevailing low level wind flow: the prevailing wind in the tropical IO changes

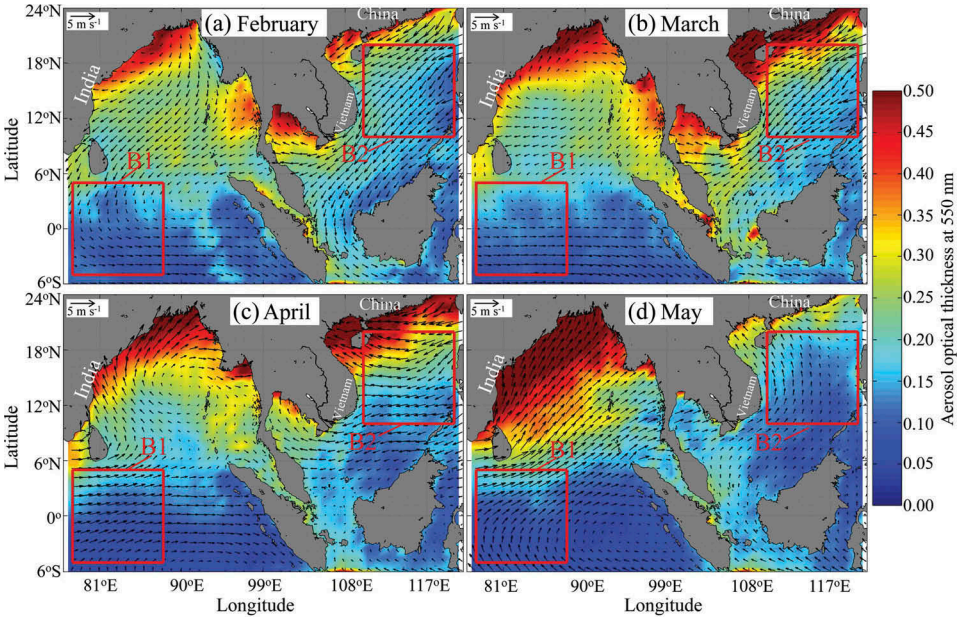

Figure 3. Monthly mean satellite AOT and wind directions in South China Sea and Indian Ocean in (*a*) February, (*b*) March, (*c*) April, and (*d*) May during 2011–2014. The colour shading indicates the AOT values and the arrows are the wind direction. The red boxes of 'B1' and 'B2' are the same as in Figure 1.

gradually from northerly and westerly in February and March to southerly and westerly in April and May, showing an increasing signal of monsoon evolution and migration northward of the Inter Tropical Convergence Zone (ITCZ) from its winter monsoon Austral position (Levy and Patoux 2010; Levy et al. 2010). Similar to the tropical IO, in SCS, northerly and easterly winds prevail in February and March, then gradually turn to southerly and easterly in April and May, with the transition from winter monsoon in February to a developing summer monsoon in May.

Detailed information of this intermonsoon evolution could be seen from the statistics of the meridional wind (only approximately 1% of the cases had a purely zonal flow) in the two sampled areas (Figure 4): The number of wind observations with a northerly component is much larger than those with a southerly component in February and March in the tropical IO [Figure 4a(*i*)]; however, southerly winds increase in frequency and dominate in April and May. The same trend with a delay in the wind evolution can be noticed in SCS, where offshore (having a northerly component) winds are dominant from February to April, but turn to be onshore (having a southerly component) in May

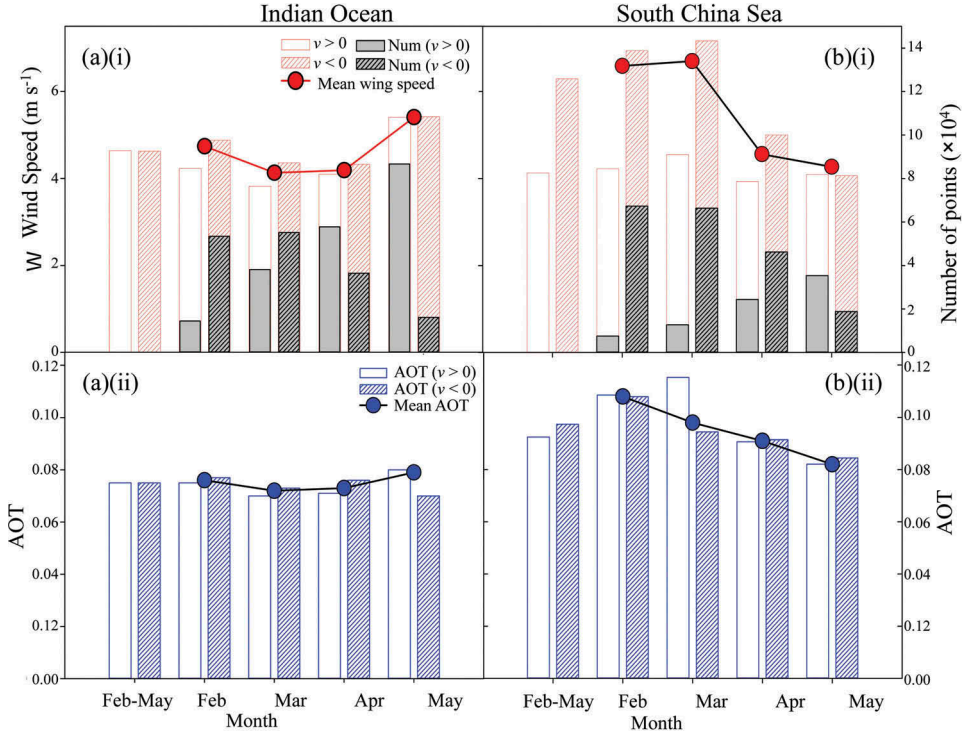

Figure 4. Statistics in tropical IO [data in 'B1' in Figures 1 and 3, (*a*) panels] and SCS [data in 'B2' in Figures 1 and 3, (*b*) panels] of [a(*i*), b(*i*)] the sampling frequency of satellite wind data under southerly ($v > 0$; primarily onshore flow in SCS and long maritime trajectories in IO) and northerly ($v < 0$; offshore flow component) wind conditions (grey bars), the corresponding mean wind speed for the intermonsoon, broken by month (red bars with patterns) and the monthly mean wind speed (indicated as red points); and [a(*ii*), b(*ii*)] AOT values from satellite under the same wind advection regimes/directions (blue bars with patterns) and monthly mean AOT (blue points) of February–May, February, March, April, and May. The legend in b(*i*) and b(*ii*) is the same as in a(*i*) and a(*ii*), respectively.

(Figure 4a(*ii*)). The overall wind speed in the tropical IO is lower than in the SCS [4.63 (standard deviation, *SD* = 2.22) m s^{-1} vs. 5.50 (*SD* = 0.68) m s^{-1}], and the speed in IO reaches a maximum [5.41 (*SD* = 2.49) m s^{-1}] in May. In contrast, the mean wind speed in February and March [6.59 (*SD* = 2.71) m s^{-1} and 6.70 (*SD* = 3.01) m s^{-1}] in SCS is higher than in April and May [4.56 (*SD* = 2.00) m s^{-1} and 4.27 (*SD* = 1.83) m s^{-1}].

Significant intraseasonal variation and spatial difference ($p \ll 0.05$) in the overall AOT datasets are found in two areas from the remote sensing data, in agreement with the results from the shipboard observations. The trend of AOT variation is similar to that of the wind speed: values are lower in the tropical IO [0.08 (*SD* = 0.04), Figure 4b(*i*)] than in SCS [0.09 (*SD* = 0.04), Figure 4b(*ii*)]; in tropical IO, AOT reach the maxima in May [0.08 (*SD* = 0.05)] when the wind is strongest [5.41 *SD* = 2.49) m s^{-1}]; and in SCS, AOT values are higher in February and March [0.11 (SD 0.05) and 0.10 (*SD* = 0.04)] when stronger winds are present [6.59 (*SD* = 2.71) and 6.70 (*SD* = 3.01) m s^{-1}], compared to April and May [0.09 (*SD* = 0.04) and 0.08 (*SD* = 0.04)] when winds are weaker [4.56 (*SD* = 2.00) and 4.27 (*SD* 1.83) m s^{-1}].

3.3.2. *Regressions of satellite AOT on wind speed in tropical IO and SCS*

The dependence of AOT on wind speed could be derived through regression and correlation models. Linear and power law relationships between AOT and wind speed were derived in numerous studies in other ocean areas (e.g. summary in Smirnov et al. 2012). Using the AOT and wind datasets selected from the two regions in SCS and tropical IO (boxes 'B1' and 'B2' in Figures 1 and 3), those relationships are derived in tropical IO and SCS. In all, AOT vary more in SCS than in the tropical IO (Figure 5), as reflected in the steeper, albeit flat, linear slopes (0.0022 and −0.0009 for SCS and IO, respectively). The relationships, either in linear (R^2 = 0.77 vs. 0.26, in SCS and IO, respectively) or power-law (R^2 = 0.90 vs. 0.62, in SCS and IO,

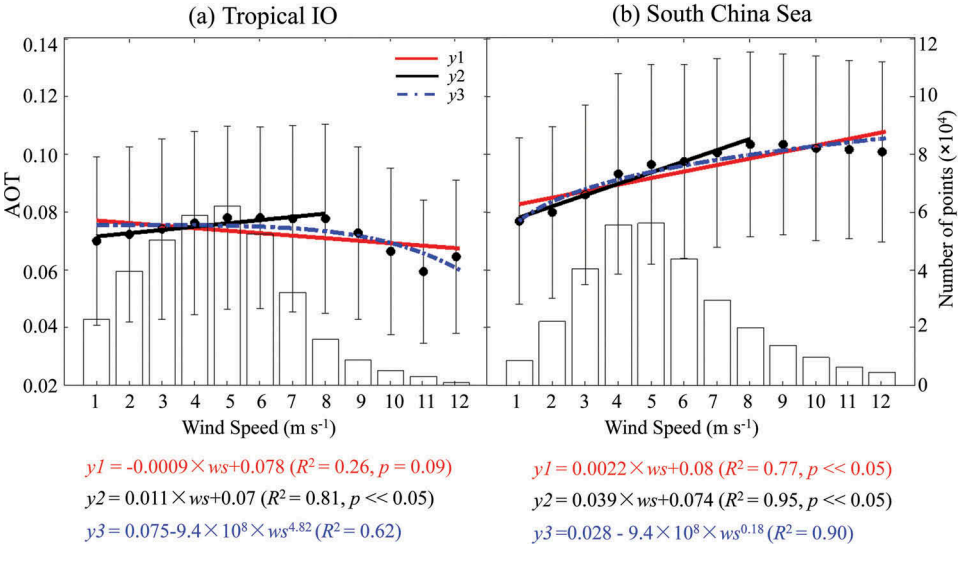

Figure 5. Regressions of satellite wind speed and AOT in (*a*) tropical IO and (*b*) SCS. Y1, y2, and y3 stand for the linear fit for wind speed less than 12 m s^{-1}, linear regression for wind speed less than 8 m s^{-1}, and power law fit for wind speed less than 12 m s^{-1}, respectively. The black circles indicate the mean AOT at corresponding wind speeds (with error bars in standard deviation), and the grey bars are the histogram of the wind speed. The legend in (*b*) is the same as in (*a*).

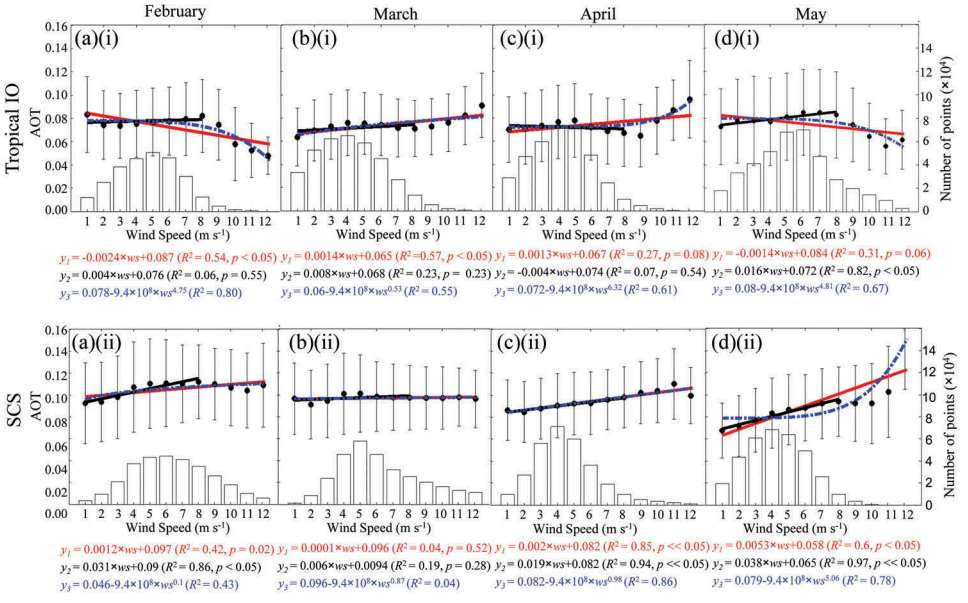

Figure 6. Regressions of satellite wind speed and AOT as in Figure 5 for tropical IO (top panels) and SCS (bottom panels), except broken by month for (*a*) February, (*b*) March, (*c*) April, and (*d*) May. Labels and makers are the same as in Figure 5.

respectively), are better in SCS than in tropical IO (Figure 5). Indeed, at the 0.05 significance level, the overall linear relationship between AOT and wind speed in the tropical IO is not significant as the *p*-value (0.09) is higher than the critical value (0.05).

From satellite datasets from February to May, in SCS, AOT increase as a function of wind speed with a very significant linear relationship (R^2 = 0.95, $p \ll 0.05$). Similar linear relationship between AOT and wind speed in tropical IO is shown (R^2 = 0.81, $p \ll 0.05$) for wind speeds of less than 8 m s^{-1}, but a decrease and scrambled relationship occurs when wind speed exceeds 8 m s^{-1} in the tropical IO (Figure 5b).

From dataset of each month, in tropical IO, good linear regressions are found (Figure 6d(*i*)) only in May (R^2 = 0.82), when wind speed <8 m s^{-1}, and the power law relationships are a little better in February (R^2 = 0.80, Figure 6a(*i*)) than in other months. The overall quality of regressions in SCS (Figure 6a(*ii*)–d(*ii*)), both linear and power law, is much better than in the tropical IO. Regressions in SCS in April and May (Figure 6c(*ii*) and d(*ii*), right) are noticeably much better than those in February and March, especially the linear relationships for wind speeds of less than 8 m s^{-1} (R^2 = 0.94 and 0.97, respectively).

4. Discussion

4.1. *Variability of AOT driving by wind differently in tropical IO and SCS*

Significant spatial and temporal variability was shown in both shipboard measured and satellite retrieved AOT data during the intermonsoon season in this study. Such variability, if not properly accounted for, will contribute much to the aerosol retrieval error in remotely sensed products because of the heterogeneity in time and space of aerosol

properties (Chatterjee et al. 2010). A key factor that determines the spatial and temporal variability of aerosol properties is the aerosol source, distribution, deposition, and transport. Wind is a main factor that affects aerosol properties, not only by generating sea salt aerosols (a major source of remote marine aerosols), but also through transporting aerosols that originate from land-based sources (Latham and Smith 1990; Smirnov et al. 1995; Vinoj et al. 2007).

In tropical IO, unlike the studies by Li and Ramanathan (2002) who found a major transition from anthropogenic aerosols during the northeasterly winter monsoon season (January–March) to mineral dust and sea salt during the southwest summer monsoon (June–August) in northern IO, our results did not show that the change in wind direction results in large anthropogenic aerosols advection into this region, probably due to our observations being farther away from land. Remote ocean background aerosol (i.e. natural particles with long residual time) is the major component during this period, and AOT value is similar to that observed by Husar, Prospero, and Stowe (1997) in remote IO from January to June. From the dependence of AOT on wind speed, both the linear regression (for wind speed <8 m s^{-1}) and the power law relationship are found to be better in May than in February, March and April. In May, westerly and southerly winds, with long fetch and trajectories over ocean only, prevail, and the mean wind speed is larger as well. As the datasets are sampled far away from land as well as aerosol composition is mostly maritime sea salts, the concentration of aerosol is more strongly related to increasing wind speed in May. Maritime background aerosols are the major component of observed AOT also in February, March, and April, and they change very little during this period because the wind speed does not change much [the corresponding slopes of the linear relationship under wind speed less than 8 m s^{-1} are very small (0.0004, 0.0008, and −0.0004, in February, March, and April, respectively)]. Therefore, increase of wind speed rather than change of prevailing wind direction are the primary cause for the variation of aerosol concentration in IO during the intermonsoon season.

In SCS, however, a distinct variation of AOT in SCS (box 'B2′ in Figure 3), especially in northern SCS, could be observed during the evolution of intermonsoon season due to the turnover of the prevailing wind direction. The high AOT along the coast of China and off the shore of Vietnam (Figures 3a and b, the upper and lower parts of 'B2′) under offshore (having a northerly component) wind in February and March turned to be very low in April and nearly disappeared in May (Figures 3c and d), when the prevailing wind changed to be onshore (having a southerly component). From the dependence of AOT on wind speed, regressions are better in April and May, when easterly and southerly (onshore) winds prevail, than those in February and March. The turnover of wind direction, accompanied by a decrease in wind speed in April and May reduces aerosol transport from land (i. e., the southern coasts of China and the Sunda Shelf that further stretches to the Gulf of Thailand), and natural marine aerosols, e.g. sea salt particles generated through wind driven sea-air fluxes, become the primary source of aerosols. Therefore, the marine aerosols show a strong dependence on wind speed, manifest as a good linear relationship between AOT and wind speed (Figures 6c(*ii*) and d(*ii*)). In contrast, the advection of land-based aerosols by the off shore wind, rather than the production of maritime aerosols, is more important in February and March resulting in lower correlations between AOT and wind speed as compared to those in April and May. Therefore, unlikely the tropical IO, the turnover of prevailing wind direction from

offshore to onshore flow resulted in less terrestrial dust and anthropogenic aerosols transport from land, and the relative 'cleaner' marine aerosols shows a stronger dependence on wind speed, which determines the variation of aerosol concentration greatly in SCS during the intermonsoon season.

4.2. *The dependence of AOT on wind speed*

From the regressions (linear or power law) of AOT and wind speed in tropical IO and SCS, AOT is noted to be enhanced linearly with increasing wind speed for wind speeds under 8 m s^{-1}, for overall datasets in both study areas, as well as data in May in tropical IO and February, April and May in SCS. As the natural marine aerosols are mostly made of sea salt particles, which are bursting off of entrained air bubbles during whitecaps formation and breaking of ocean wave crests (Andreas 1998; O'Dowd and De Leeuw 2007; Huang, Thomas, and Grainger 2010), and as white caps generally start to appear at wind speed range of 7–8 m s^{-1}, i.e. the Beaufort Scale (Isemer and Hasse 1991; Banner, Babanin, and Young 2000; Babanin et al. 2001), we see this peak in AOT at 8 m s^{-1}.

However, a reduction in the slope of the AOT-wind speed relationship is found in tropical IO, when wind speed is greater than 8 m s^{-1}, as compared to a slight reduction of the rate of increase in other studies (Figure 7). This reduction is possibly a reflection of the near absence of AOT retrievals at high wind speeds, which greatly impacts the quality and

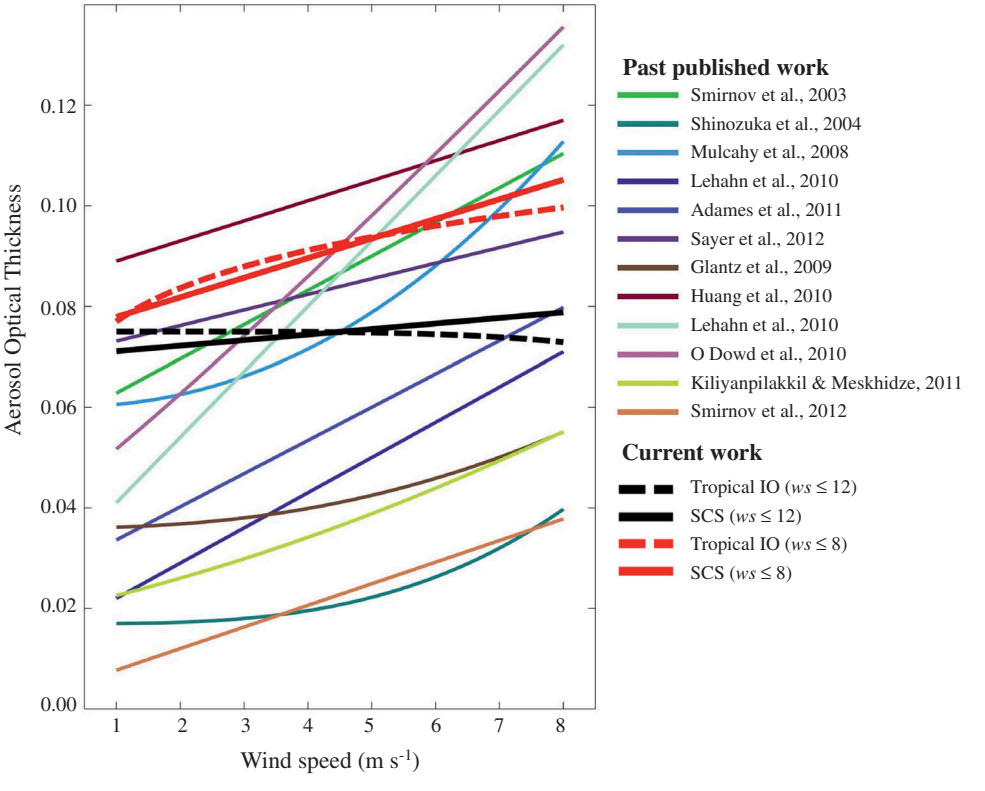

Figure 7. AOT as a function of wind speed in the present study (red and black curves), compared to other studies (see Table 3 from Smirnov et al. 2012).

significance of the regression at these wind speeds. Two possible reasons are accounting for this absence of aerosols. One reason could be the insufficient AOT data when wind speeds were over 8 m s^{-1} which could not satisfy the statistical relationship between AOT and wind speed. The statistical AOT samples in Indian Ocean when wind speeds were between 8 and 12 m s^{-1} were much less than those wind speeds were between 0 and 4 m s^{-1} and wind speeds were between 4 and 8 m s^{-1} (20,659 vs. 166,057 and 207,497, respectively, Figure 5a), and about half of those datasets distributed the range between 8 and 9 m s^{-1}. According to the normal distribution theory, the valid number of AOT values of wind speeds between 8 and 12 m s^{-1} should not be less than 23,810 (6.04% of 394,213 at $p = 0.05$), which indicate that the number of AOT data when wind speeds were over 8 m s^{-1} are too small to derive the regression. The average wind speed of these four months is 4.74, 4.13, 4.19, and 5.41 m s^{-1} respectively (Figure 4a(*i*)), which indicates the absence of aerosols under high wind speed as well. The other reason could be the decrease of aerosol number concentration. It has been reported that the scavenging of aerosols occurs because of larger seawater dropping injected into the atmosphere at high wind speeds, and would act as a built-in sink to restrict the enhancement in concentration of marine aerosols at high wind speeds (Pant, Deshpande, and Kamra 2008; Kiliyanpilakkil and Meskhidze 2011). The first reason is more likely to response for the absence of the aerosols when wind speeds are greater than 8 m s^{-1}, as scavenging of aerosols generally occurs at wind speeds which are above 16 m s^{-1}.

4.3. *Discrepancy between shipboard measurements and satellite data*

When calibrating MODIS-Aqua AOT data with shipboard measurements, an overall good agreement is found between the shipboard and MODIS-Aqua AOT (Figure 2a) both in the tropical IO and SCS, but there exists a clear spatial difference: agreement is better in Equatorial belt than Non-Equatorial area (Figures 2a and b). Other than the overall lower AOT values, the smaller diurnal variation in AOT in IO compared to that in SCS, as well as in Non-Equatorial area, is the reason for the smaller difference between shipboard and satellite observations.

As a polar-orbiting satellite observes a given area only once or twice each day, the diurnal variation of AOT is not available from satellite observations. Thus, a smaller diurnal variation in the IO (0.07 ± 0.01, Table 2), as compared to the SCS (0.11 ± 0.02), results in a closer agreement between shipboard and satellite AOT observations there (and in other locations with a small diurnal variation), and a greater diurnal variation as observed in SCS and in the Non-Equatorial area (0.10 ± 0.01) should result in a larger error. This has broader implications to satellite retrievals of AOT, as well as other parameters (e.g. wind speed (Hedin et al. 1991; Tomita and Kubota 2011), water vapour (Tian et al. 2004), tropospheric temperature (Mears and Wentz 2005), in areas where large diurnal variation exists or is expected, and corrections for this effect may be required especially when calibrating satellite datasets with in-situ data in such areas.

The smaller diurnal variation is only partly responsible for the larger errors (differences between shipboard measurements and satellite retrievals) present away from the equator and in the SCS. Another cause for discrepancy is related to the smaller values of AOT_N compared to AOT_{NE} and those of AOT in IO compared to the SCS that were observed in both shipboard measurements and satellite data. The matched AOT values

in the Equatorial belt have a smaller and less variation than those in Non-Equatorial area (Figure 2b). The shipboard observed AOT in SCS is also clearly higher than in IO (0.16 ± 0.01 in SCS vs. 0.13 ± 0.01 in IO. It has been reported that the MODIS tends to underestimate (when validated against *in situ* AOT measurements) for high AOT (Jiang et al. 2007; Liu et al. 2007; Xiao et al. 2009). Therefore, greater values would result in a higher retrieval error.

5. Summary and conclusions

Based on analysis of shipboard and satellite data during 2011–2014, the present study discusses, for the first time, the variability of AOT in both SCS and the tropical IO during the intermonsoon season (February–May) along with the mechanisms driving it. The conclusions can be drawn from this work are as follows:

(1) A strong intraseasonal variability of AOT, primarily driven by changes in the prevailing wind during the monsoon evolution, is observed in both shipboard and satellite data in both tropical IO and SCS.
(2) The AOT has a significant dependence on wind speed, especially when <8 m s^{-1}. Dependence of AOT on wind speed exhibits intraseasonal differences: it is stronger in the tropical IO in May when strong winds with longer maritime trajectories prevail, and in April and May in SCS when onshore winds prevail.
(3) Aerosols in tropical IO and SCS are driven by and respond differently to the changing prevailing wind. In the tropical IO, AOT varied little under low wind speed conditions (February–April) but increased at higher wind speeds in May, as aerosols are mostly natural marine components, and its concentration increases due to the enhanced bubble-breaking activity at the sea surface and increased entrainment of sea-salt particles under high wind speed. In SCS, in contrast, the turnover from offshore to onshore flow resulted in less terrestrial dust and anthropogenic aerosols transport from land, and the relative 'cleaner' marine aerosols shows a stronger dependence on wind speed.
(4) The agreement between shipboard and satellite AOT is better in Equatorial belt (5° S–5° N, i.e. remote area of the tropical IO) than Non-Equatorial area (5° N–25° N), and could be explained by the lower AOT values and the smaller diurnal variation near the Equator.

Acknowledgments

The shipboard AOT data in this study are available on the Maritime Aerosol Network website (http://aeronet.gsfc.nasa.gov/new_web/maritime_aerosol_network.html). The satellite AOT data used in this work are available from NASA Giovanni (http://giovanni.gsfc.nasa.gov) and NASA's Ocean Colour Web (http://oceancolor.gsfc.nasa.gov/cgi/l3), and wind data of ASCAT from the Remote Sensing Systems (http://www.remss.com/). We appreciate Dr Alexander Smirnov for his kind help with data processing and transfer calibration, and Dr Naoto Ebuchi (Hokkaido University) for his useful advice on the interpretation of data. We thank the science party and crew of the R/V Shiyan1 (SCSIO, CAS) for their support and technical assistance, especially Jingrou Lin, Jing Sun and YongJun Song.

The present work was supported by State Key Laboratory of Tropical Oceanography and Guangdong Key Laboratory of Ocean remote Sensing (LORS), South China Sea Institute of Oceanology Chinese Academy of Sciences (Project No. LTO1604 and LORS1701), and funding from South China Sea Branch of State Oceanic Administration (1606), National Natural Sciences Foundation of China (41430968, 41106105), Research Project of Collaborative Innovation Center for 21st-Century Maritime Silk Road Studies (2015HS05), and China Petroleum & Chemical Corporation (313099) awarded to DL Tang, and US National Science Foundation (ATM - 0741832), and Chinese Academy of Sciences program for visiting professorships for senior international scientists (Grant 2013T1Z0048 at South China Sea Institute of Oceanology) awarded to G. Levy.

Disclosure statement

No potential conflict of interest was reported by the authors.

Funding

This work was supported by the Chinese Academy of Sciences program for visiting professorships for senior international scientists [2013T1Z0048]; US National Science Foundation [ATM – 0741832]; Funding of South China Sea Branch of State Oceanic Administration [1606]; National Natural Sciences Foundation of China [41106105, 41430968]; Open Research Program: State Key Laboratory of Tropical Oceanography and Guangdong Key Laboratory of Ocean remote Sensing (LORS); South China Sea Institute of Oceanology Chinese Academy of Sciences [LTO1604 and LORS1701]; Research Project of Collaborative Innovation Center for 21st-Century Maritime Silk Road Studies [2015HS05], and China Petroleum & Chemical Corporation [313099].

References

Andreas, E. L. 1998. "A New Sea Spray Generation Function for Wind Speeds up to 32m S^{-1}." *Journal of Physical Oceanography* 28 (11): 2175–2184. doi:10.1175/1520-0485(1998)028<2175:Anssgf>2.0.Co;2.

Babanin, A. R., and M. L. Banner. 2001. "Breaking Probabilities for Dominant Surface Waves on Water of Finite Constant Depth." *Journal of Geophysical Research: Oceans* 106 (C6): 11659–11676. doi:10.1029/2000jc000215.

Banner, M. L., A. V. Babanin, and L. R. Young. 2000. "Breaking Probability for Dominant Waves on the Sea Surface." *Journal of Physical Oceanography* 30 (12): 3145–3160. doi:10.1175/1520-0485(2000)030<3145:bpfdwo>2.0.co;2.

Barnett, T. P., J. C. Adam, and D. P. Lettenmaier. 2005. "Potential Impacts of a Warming Climate on Water Availability in Snow-Dominated Regions." *Nature* 438 (7066): 303–309. doi:10.1038/Nature04141.

Capone, D. G., J. P. Zehr, H. W. Paerl, B. Bergman, and E. J. Carpenter. 1997. "Trichodesmium, a Globally Significant Marine Cyanobacterium." *Science* 276 (5316): 1221–1229. doi:10.1126/science.276.5316.1221.

Charlson, R. J., S. E. Schwartz, J. M. Hales, R. D. Cess, J. A. Coakley, J. E. Hansen, and D. J. Hofmann. 1992. "Climate Forcing by Anthropogenic Aerosols." *Science* 255 (5043): 423–430. doi:10.1126/science.255.5043.423.

Chatterjee, A., A. M. Michalak, R. A. Kahn, S. R. Paradise, A. J. Braverman, and C. E. Miller. 2010. "A Geostatistical Data Fusion Technique for Merging Remote Sensing and Ground-Based Observations of Aerosol Optical Thickness." *Journal of Geophysical Research:Atmospheres* 115. doi:10.1029/2009jd013765.

Chen, W., H. F. Graf, and R. H. Huang. 2000. "The Interannual Variability of East Asian Winter Monsoon and Its Relation to the Summer Monsoon." *Advances in Atmospheric Sciences* 17 (1): 48–60. doi:10.1007/s00376-000-0042-5.

Dai, A., K. E. Trenberth, and T. R. Karl. 1999. "Effects of Clouds, Soil Moisture, Precipitation, and Water Vapor on Diurnal Temperature Range." *Journal of Climate* 12 (8): 2451–2473. doi:10.1175/1520-0442(1999)012<2451:Eocsmp>2.0.Co;2.

de Baar, H. J. W., J. T. M. de Jong, D. C. E. Bakker, B. M. Loscher, C. Veth, U. Bathmann, and V. Smetacek. 1995. "Importance of Iron for Plankton Blooms and Carbon Dioxide Drawdown in the Southern Ocean." *Nature* 373 (6513): 412–415. doi:10.1038/373412a0.

DeWitt, H. L., D. J. Coffman, K. J. Schulz, W. A. Brewer, T. S. Bates, and P. K. Quinn. 2013. "Atmospheric Aerosol Properties over the Equatorial Indian Ocean and the Impact of the Madden-Julian Oscillation." *Journal of Geophysical Research-Atmospheres* 118 (11): 5736–5749. doi:10.1002/Jgrd.50419.

Ding, Y. H., and J. C. L. Chan. 2005. "The East Asian Summer Monsoon: An Overview." *Meteorology and Atmospheric Physics* 89 (1–4): 117–142. doi:10.1007/s00703-005-0125-z.

Eck, T. F., B. N. Holben, J. S. Reid, O. Dubovik, A. Smirnov, N. T. O'Neill, I. Slutsker, and S. Kinne. 1999. "Wavelength Dependence of the Optical Depth of Biomass Burning, Urban, and Desert Dust Aerosols." *Journal of Geophysical Research-Atmospheres* 104 (D24): 31333–31349. doi:10.1029/1999jd900923.

Figasaldaña, J., J. J. W. Wilson, E. Attema, R. Gelsthorpe, M. R. Drinkwater, and A. Stoffelen. 2002. "The Advanced Scatterometer (ASCAT) on the Meteorological Operational (Metop) Platform: A Follow on for European Wind Scatterometers." *Canadian Journal of Remote Sensing* 28 (3): 404–412. doi:10.1109/IGARSS.2012.6350966.

Fitzgerald, J. W. 1991. "Marine Aerosols: A Review." *Atmospheric Environment. Part A. General Topics* 25 (3–4): 533–545. doi:10.1016/0960-1686(91)90050-H.

Friedman, J. H., J. L. Bentley, and R. A. Finkel. 1977. "An Algorithm for Finding Best Matches in Logarithmic Expected Time." *ACM Trans. Math. Softw.* 3 (3): 209–226. doi:10.1145/355744.355745.

Glantz, P., E. D. Nilsson, and W. von Hoyningen-Huene. 2009. "Estimating a Relationship between Aerosol Optical Thickness and Surface Wind Speed over the Ocean." *Atmospheric Research* 92 (1): 58–68. doi:10.1016/j.atmosres.2008.08.010.

Guo, C., J. Yu, T. Y. Ho, L. Wang, S. Song, L. Kong, and H. Liu. 2012. "Dynamics of Phytoplankton Community Structure in the South China Sea in Response to the East Asian Aerosol Input." *Biogeosciences* 9 (4): 1519–1536. doi:10.5194/bg-9-1519-2012.

Hansen, J., M. Sato, and R. Ruedy. 1995. "Long-Term Changes of the Diurnal Temperature Cycle - Implications about Mechanisms of Global Climate-Change." *Atmospheric Research* 37 (1–3): 175–209. doi:10.1016/0169-8095(94)00077-Q.

Hedin, A. E., M. A. Biondi, R. G. Burnside, G. Hernandez, R. M. Johnson, T. L. Killeen, C. Mazaudier, et al. 1991. "Revised Global-Model of Thermosphere Winds Using Satellite and Ground-Based Observations." *Journal of Geophysical Research-Space Physics* 96 (A5): 7657–7688. doi:10.1029/91ja00251.

Holben, B. N., T. F. Eck, I. Slutsker, D. Tanre, J. P. Buis, A. Setzer, E. Vermote, et al. 1998. "AERONET - A Federated Instrument Network and Data Archive for Aerosol Characterization." *Remote Sensing of Environment* 66 (1): 1–16. doi:10.1016/S0034-4257(98)00031-5.

Huang, H., G. E. Thomas, and R. G. Grainger. 2010. "Relationship between Wind Speed and Aerosol Optical Depth over Remote Ocean." *Atmospheric Chemistry and Physics* 10 (13): 5943–5950. doi:10.5194/acp-10-5943-2010.

Huang, Y., R. E. Dickinson, and W. L. Chameides. 2006. "Impact of Aerosol Indirect Effect on Surface Temperature over East Asia." *Proceedings of the National Academy of Sciences of the United States of America* 103 (12): 4371–4376. doi:10.1073/pnas.0504428103.

Husar, R. B., J. M. Prospero, and L. L. Stowe. 1997. "Characterization of Tropospheric Aerosols over the Oceans with the NOAA Advanced Very High Resolution Radiometer Optical Thickness Operational Product." *Journal of Geophysical Research* 102 (102): 16889–16909. doi:10.1029/96JD04009.

Ichoku, C., R. Levy, Y. J. Kaufman, L. A. Remer, R. R. Li, V. J. Martins, B. N. Holben, et al. 2002. "Analysis of the Performance Characteristics of the Five-Channel Microtops II Sun Photometer for Measuring Aerosol Optical Thickness and Precipitable Water Vapor." *Journal of Geophysical Research-Atmospheres* 107 (D13). doi:10.1029/2001jd001302.

Isemer, H. J., and L. Hasse. 1991. "The Scientific Beaufort Equivalent Scale - Effects on Wind Statistics and Climatological Air Sea Flux Estimates in the North-Atlantic Ocean." *Journal of Climate* 4 (8): 819–836. doi:10.1175/1520-0442(1991)004<0819:Tsbese>2.0.Co;2.

Jiang, X., Y. Liu, B. Yu, and M. Jiang. 2007. "Comparison of MISR Aerosol Optical Thickness with AERONET Measurements in Beijing Metropolitan Area." *Remote Sensing of Environment* 107 (1–2): 45–53. doi:10.1016/j.rse.2006.06.022.

Kiliyanpilakkil, V. P., and N. Meskhidze. 2011. "Deriving the Effect of Wind Speed on Clean Marine Aerosol Optical Properties Using the A-Train Satellites." *Atmospheric Chemistry and Physics* 11 (22): 11401–11413. doi:10.5194/acp-11-11401-2011.

Latham, J., and M. H. Smith. 1990. "Effect on Global Warming of Wind-Dependent Aerosol Generation at the Ocean Surface." *Nature* 347 (6291): 372–373. doi:10.1038/347372a0.

Lau, K. M., and S. Yang. 1997. "Climatology and Interannual Variability of the Southeast Asian Summer Monsoon." *Advances in Atmospheric Sciences* 14 (2): 141–162. doi:10.1007/s00376-997-0016-y.

Lee, K. H., Y. J. Kim, W. von Hoyningen-Huene, and J. P. Burrow. 2007. "Spatio-Temporal Variability of Satellite-Derived Aerosol Optical Thickness over Northeast Asia in 2004." *Atmospheric Environment* 41 (19): 3959–3973. doi:10.1016/j.atmosenv.2007.01.048.

Levy, G., A. Geiss, and M. R. Ramesh Kumar. 2010. "Near-Equatorial Convective Regimes over the Indian Ocean as Revealed by Synergistic Analysis of Satellite Observations." *Advances in Geosciences* 22 (22): 101–114. doi:10.1080/01431161.2010.485153.

Levy, G., and J. Patoux. 2010. "Indian Ocean Near-Equatorial Symmetric Stability from Satellite Observations: An Elusive Connection to Atmospheric Convection." *International Journal of Remote Sensing* 31 (17–18): 4665–4681. doi:10.1080/01431161.2010.485153.

Levy, G., and R. A. Brown. 1986. "A Simple, Objective Analysis Scheme for Scatterometer Data." *Journal of Geophysical Research: Oceans* 91 (C4): 5153–5158. doi:10.1029/JC091iC04p05153.

Li, F., and V. Ramanathan. 2002. "Winter to Summer Monsoon Variation of Aerosol Optical Depth over the Tropical Indian Ocean." *Journal of Geophysical Research: Atmospheres* 107 (D16): AAC 2-1-AAC 2-13. doi:10.1029/2001jd000949.

Liepert, B., and I. Tegen. 2002. "Multidecadal Solar Radiation Trends in the United States and Germany and Direct Tropospheric Aerosol Forcing." *Journal of Geophysical Research-Atmospheres* 107 (D12). doi:10.1029/2001jd000760.

Liepert, B. G., J. Feichter, U. Lohmann, and E. Roeckner. 2004. "Can Aerosols Spin down the Water Cycle in a Warmer and Moister World?" *Geophysical Research Letters* 31 (6). doi:10.1029/2003gl019060.

Lin, I. I., G. T. F. Wong, C. C. Lien, C. Y. Chien, C. W. Huang, and J. P. Chen. 2009. "Aerosol Impact on the South China Sea Biogeochemistry: An Early Assessment from Remote Sensing." *Geophysical Research Letters* 36. doi:10.1029/2009gl037484.

Lin, I. I., J. P. Chen, G. T. F. Wong, C. W. Huang, and C. C. Lien. 2007. "Aerosol Input to the South China Sea: Results from the MODerate Resolution Imaging Spectro-Radiometer, the Quick Scatterometer, and the Measurements of Pollution in the Troposphere Sensor." *Deep-Sea Research Part Ii-Topical Studies in Oceanography* 54 (14–15): 1589–1601. doi:10.1016/j.dsr2.2007.05.013.

Liu, K. K., S. Y. Chao, P. T. Shaw, G. C. Gong, C. C. Chen, and T. Y. Tang. 2002. "Monsoon-Forced Chlorophyll Distribution and Primary Production in the South China Sea: Observations and a Numerical Study." *Deep-Sea Research Part I-Oceanographic Research Papers* 49 (8): 1387–1412. doi:10.1016/S0967-0637(02)00035-3.

Liu, Y., M. Franklin, R. Kahn, and P. Koutrakis. 2007. "Using Aerosol Optical Thickness to Predict Ground-Level PM2.5 Concentrations in the St. Louis Area: A Comparison between MISR and MODIS." *Remote Sensing of Environment* 107 (1–2): 33–44. doi:10.1016/j.rse.2006.05.022.

Mears, C. A., and F. J. Wentz. 2005. "The Effect of Diurnal Correction on Satellite-Derived Lower Tropospheric Temperature." *Science* 309 (5740): 1548–1551. doi:10.1126/science.1114772.
Menon, H. B., N. Sangekar, A. Lotliker, K. K. Moorthy, and P. Vethamony. 2011. "Aerosol Optical Thickness and Spatial Variability along Coastal and Offshore Waters of the Eastern Arabian Sea." *Ices Journal of Marine Science* 68 (4): 745–750. doi:10.1093/icesjms/fsq191.
Moorthy, K. K., S. K. Satheesh, and B. V. K. Murthy. 1997. "Investigations of Marine Aerosols over the Tropical Indian Ocean." *Journal of Geophysical Research: Atmospheres* 102 (D15): 18827–18842. doi:10.1029/97jd01121.
Morys, M., F. M. Mims, S. Hagerup, S. E. Anderson, A. Baker, J. Kia, and T. Walkup. 2001. "Design, Calibration, and Performance of MICROTOPS II Handheld Ozone Monitor and Sun Photometer." *Journal of Geophysical Research-Atmospheres* 106 (D13): 14573–14582. doi:10.1029/2001jd900103.
Mulcahy, J. P., C. D. O'Dowd, S. G. Jennings, and D. Ceburnis. 2008. "Significant Enhancement of Aerosol Optical Depth in Marine Air under High Wind Conditions." *Geophysical Research Letters* 35 (16). doi:10.1029/2008gl034303.
O'Dowd, C. D., and G. De Leeuw. 2007. "Marine Aerosol Production: A Review of the Current Knowledge." *Philosophical Transactions of the Royal Society a-Mathematical Physical and Engineering Sciences* 365 (1856): 1753–1774. doi:10.1098/rsta.2007.2043.
Paerl, H. W. 1997. "Coastal Eutrophication and Harmful Algal Blooms: Importance of Atmospheric Deposition and Groundwater as "New" Nitrogen and Other Nutrient Sources." *Limnology and Oceanography* 42 (5): 1154–1165. doi:10.4319/lo.1997.42.5_part_2.1154.
Pant, V. C., G. Deshpande, and A. K. Kamra. 2008. "On the Aerosol Number Concentration–Wind Speed Relationship during a Severe Cyclonic Storm over South Indian Ocean." *Journal of Geophysical Research: Atmospheres* 113 (D2): D02206. doi:10.1029/2006jd008035.
Penner, J. E., R. E. Dickinson, and C. A. Oneill. 1992. "Effects of Aerosol from Biomass Burning on the Global Radiation Budget." *Science* 256 (5062): 1432–1434. doi:10.1126/science.256.5062.1432.
Porter, J. N., M. Miller, C. Pietras, and C. Motell. 2001. "Ship-based Sun Photometer Measurements using Microtops Sun Photometers" *Journal of Atmospheric & Oceanic Technology* 18 (5): 765–774. doi:10.1175/1520-0426(2001)018<0765:sbspmu>2.0.Co;2.
Ramanathan, V., P. J. Crutzen, J. Lelieveld, A. P. Mitra, D. Althausen, J. Anderson, M. O. Andreae, et al. 2001b. "Indian Ocean Experiment: An Integrated Analysis of the Climate Forcing and Effects of the Great Indo-Asian Haze." *Journal of Geophysical Research-Atmospheres* 106 (D22): 28371–28398. doi:10.1029/2001jd900133.
Ramanathan, V., P. J. Crutzen, J. T. Kiehl, and D. Rosenfeld. 2001a. "Atmosphere - Aerosols, Climate, and the Hydrological Cycle." *Science* 294 (5549): 2119–2124. doi:10.1126/science.1064034.
Remer, L. A., D. Tanre, Y. J. Kaufman, C. Ichoku, S. Mattoo, R. Levy, D. A. Chu, et al. 2002. "Validation of MODIS Aerosol Retrieval over Ocean." *Geophysical Research Letters* 29 (12). doi:10.1029/2001gl013204.
Remer, L. A., Y. J. Kaufman, and R. G. Kleidman. 2006. "Comparison of Three Years of Terra and Aqua MODIS Aerosol Optical Thickness over the Global Oceans." *Ieee Geoscience and Remote Sensing Letters* 3 (4): 537–540. doi:10.1109/Lgrs.2006.879562.
Ricciardulli, L., T. Meissner, and F. Wentz. 2012. "Towards a Climate Data Record of Satellite Ocean Vector Winds." *Geoscience and Remote Sensing Symposium IEEE* 88 (60): 2067–2069. doi:10.1109/IGARSS.2012.6350966.
Salim, M., and A. K. Mishra. 2013. "Seasonality and Latitudinal Variation of Water Vapour and Aerosol Optical Thickness and Their Relationship over Tropical Indian Ocean." *Journal of the Indian Society of Remote Sensing* 41 (2): 279–290. doi:10.1007/s12524-012-0222-7.
Smirnov, A., A. M. Sayer, B. N. Holben, N. C. Hsu, S. M. Sakerin, A. Macke, N. B. Nelson, et al. 2012. "Effect of Wind Speed on Aerosol Optical Depth over Remote Oceans, Based on Data from the Maritime Aerosol Network." *Atmospheric Measurement Techniques* 5 (2): 377–388. doi:10.5194/amt-5-377-2012.
Smirnov, A., B. N. Holben, I. Slutsker, D. M. Giles, C. R. McClain, T. F. Eck, S. M. Sakerin, et al. 2009. "Maritime Aerosol Network as a Component of Aerosol Robotic Network." *Journal of Geophysical Research-Atmospheres* 114. doi:10.1029/2008jd011257.

Smirnov, A., B. N. Holben, O. Dubovik, R. Frouin, T. F. Eck, and I. Slutsker. 2003a. "Maritime Component in Aerosol Optical Models Derived from Aerosol Robotic Network Data." *Journal of Geophysical Research-Atmospheres* 108 (D1). doi:10.1029/2002jd002701.

Smirnov, A., B. N. Holben, T. F. Eck, O. Dubovik, and I. Slutsker. 2003b. "Effect of Wind Speed on Columnar Aerosol Optical Properties at Midway Island." *Journal of Geophysical Research-Atmospheres* 108 (D24). doi:10.1029/2003jd003879.

Smirnov, A., Y. Villevalde, N. T. O'Neill, A. Royer, and A. Tarussov. 1995. "Aerosol Optical Depth over the Oceans: Analysis in Terms of Synoptic Air Mass Types." *Journal of Geophysical Research: Atmospheres* 100 (D8): 16639–16650. doi:10.1029/95jd01265.

Tian, Y., R. E. Dickinson, L. Zhou, X. Zeng, Y. Dai, R. B. Myneni, Y. Knyazikhin, et al. 2004. "Comparison of Seasonal and Spatial Variations of Leaf Area Index and Fraction of Absorbed Photosynthetically Active Radiation from Moderate Resolution Imaging Spectroradiometer (MODIS) and Common Land Model." *Journal of Geophysical Research-Atmospheres* 109 (D1). doi:10.1029/2003jd003777.

Timmermans, K. R., L. J. A. Gerringa, H. J. W. de Baar, B. van der Wagt, M. J. W. Veldhuis, J. T. M. de Jong, P. L. Croot, and M. Boye. 2001. "Growth Rates of Large and Small Southern Ocean Diatoms in Relation to Availability of Iron in Natural Seawater." *Limnology and Oceanography* 46 (2): 260–266. doi:10.4319/lo.2001.46.2.0260.

Tomita, H., and M. Kubota. 2011. "Sampling Error of Daily Mean Surface Wind Speed and Air Specific Humidity Due to Sun-Synchronous Satellite Sampling and Its Reduction by Multi-Satellite Sampling." *International Journal of Remote Sensing* 32 (12): 3389–3404. doi:10.1080/01431161003749428.

Tseng, C. M., G. T. F. Wong, I. I. Lin, C. R. Wu, and K. K. Liu. 2005. "A Unique Seasonal Pattern in Phytoplankton Biomass in Low-Latitude Waters in the South China Sea." *Geophysical Research Letters* 32 (8). doi:10.1029/2004GL022111.

Vinoj, V., A. Anjan, M. Sudhakar, S. K. Satheesh, J. Srinivasan, and K. K. Moorthy. 2007. "Latitudinal Variation of Aerosol Optical Depths from Northern Arabian Sea to Antarctica." *Geophysical Research Letters* 34 (10). doi:10.1029/2007gl029419.

Wong, G. T. F., T. L. Ku, M. Mulholland, C. M. Tseng, and D. P. Wang. 2007. "The SouthEast Asian Time-Series Study (SEATS) and the Biogeochemistry of the South China Sea - an Overview." *Deep-Sea Research Part Ii-Topical Studies in Oceanography* 54 (14–15): 1434–1447. doi:10.1016/j.dsr2.2007.05.012.

Xiao, N. C., T. Shi, C. A. Calder, D. K. Munroe, C. Berrett, S. Wolfinbarger, and D. M. Li. 2009. "Spatial Characteristics of the Difference between MISR and MODIS Aerosol Optical Depth Retrievals over Mainland Southeast Asia." *Remote Sensing of Environment* 113 (1): 1–9. doi:10.1016/j.rse.2008.07.011.

Yuan, W., and J. Zhang. 2006. "High Correlations between Asian Dust Events and Biological Productivity in the Western North Pacific." *Geophysical Research Letters* 33 (7). doi:10.1029/2005gl025174.

Zhang, J. L., and J. S. Reid. 2006. "MODIS Aerosol Product Analysis for Data Assimilation: Assessment of Over-Ocean Level 2 Aerosol Optical Thickness Retrievals." *Journal of Geophysical Research-Atmospheres* 111 (D22). doi:10.1029/2005jd006898.